2008

Design Optimization of Electrostatically Actuated Minature Compressors for Electronics Cooling

Abhijit Sathe
Purdue University

Eckhard Groll
Purdue University

Suresh Garimella
Purdue University, sureshg@purdue.edu

DESIGN OPTIMIZATION OF ELECTROSTATICALLY ACTUATED MINIATURE COMPRESSORS FOR ELECTRONICS COOLING

Abhijit A Sathe, Eckhard A Groll* and Suresh V Garimella
Cooling Technologies Research Center, School of Mechanical Engineering
Purdue University, West Lafayette, Indiana 47907, USA

* Corresponding author, email: groll@purdue.edu

ABSTRACT

This paper presents a feasibility study of using electrostatically actuated diaphragm compressors for use in a miniature scale refrigeration system for electronics cooling. An experimentally validated analytical model for the diaphragm compressor has already been developed. The dimensions for the diaphragm compressor are selected based on an analytical optimization theory developed in this paper. Based on the diaphragm compressor analysis, the pressure rise and volume flow rate required for cooling of modern electronics may not be achieved using a single compressor unit because of the material property limitations. Hence, a 3-D array of the compressor has been proposed for satisfying the pressure rise and the volume flow rate requirements. It is shown that with this array, it is theoretically possible for the compressor to fulfill the cooling requirements and yet fit within the size restrictions set by the electronics cooling industry.

1. INTRODUCTION

With the advent of high-speed and ultra-compact performance notebook computers and the ever increasing heat generation in the CPUs, GPUs, memory modules and disk drives, the heat dissipation challenges are more difficult than ever. Traditional electronics cooling approaches such as forced convective air cooling using conventional heat sinks are soon expected to reach their limits for meeting the dissipation needs of these emerging high-performance electronics systems (Krishnan et al., 2007). Alternative electronics cooling approaches include heat pipes, liquid immersion, jet impingement and sprays, microchannel heat sinks, thermoelectric cooling, and refrigeration (Garimella, 2006). Vapor compression refrigeration appears to be among the more promising techniques because of its ability to operate at varying loads and high ambient temperatures. A schematic of a vapor compression refrigeration system for electronics cooling is shown in Figure 1. The advantages of refrigeration cooling over conventional techniques are (Phelan, 2001): (a) maintenance of low junction temperatures while dissipating high heat fluxes, (b) potential increase in microprocessor performance at lower operating temperatures, and (c) increased chip reliability. However, these advantages must be balanced against the following drawbacks: (a) increased complexity and cost of the cooling system, (b) a possible increase in cooling system volume, and (b) uncertainties in the system reliability due to the moving parts in the compressor.

Over the past few years, several researchers have investigated the feasibility of using miniature-scale vapor compression refrigeration systems for microprocessor cooling. A vapor-compression system model for electronics cooling based on thermodynamic and heat transfer considerations was developed by Bash (2001). Cycle components were analyzed by combining the principles of thermodynamics and heat transfer in order to account for irreversibilities inherent in practical system. A conventional vapor compression system consisting of a serpentine evaporator, an intercooler, a compressor, a plate fin-and-tube condenser, and a capillary tube expansion device was tested. The modeling results were validated against the test results with accuracy on the COP predictions within ± 8 % for heat loads between 210 and 400 W.

Heydari (2002) developed a steady-state simulation model of a refrigeration cycle for cooling of computers based on four sub-models of the cooling system consisting of a free-piston linear compressor, a compact condenser, a capillary tube, and a cold plate evaporator. The model was based on a simple thermodynamic control volume approach and semi-empirical mass flow rate correlations for capillary tubes. It also used a lumped method to calculate the heat transfer rate and empirical correlations to estimate the pressure drop in the condenser.

Mongia et al. (2006) developed one of the first miniature refrigeration systems for cooling of high-power components in a notebook computer. Their system employed small component prototypes specifically designed for a notebook form factor, including a microchannel condenser, a microchannel cold plate evaporator, and a miniature-scale linear piston compressor. Isobutane was used as a refrigerant for the prototype system that achieved a cooling rate of approximately 50 W and a system COP of approximately 2.25. The overall isentropic efficiency of the linear compressor was measured as 33 to 35%. Information on the reliability of the linear compressor was not provided. A simulation model for analysis and optimization of the compressor or the refrigeration cycle was also not developed.

The feasibility and potential of miniature vapor compression refrigeration systems for electronics cooling were studied by Cremaschi et al. (2007). A detailed review of the recent small-scale refrigeration systems, their performance potential and challenges were discussed. The authors concluded that efficient and reliable mini- and micro-compressors are essential in order to achieve energy efficiencies that would render refrigeration systems competitive with other electronics cooling technologies.

Trutassanawin et al. (2006) experimentally tested a small-scale refrigeration system consisting of a commercially available miniature-scale compressor, a microchannel condenser and a cold plate evaporator. The system achieved a maximum cooling capacity of 226 W while maintaining the maximum CPU temperature at 53°C. The system performance was found to strongly depend on the compressor efficiencies. The overall isentropic and volumetric efficiencies of this compressor, which was not designed for electronics cooling applications, were as low as 25% and 50%, respectively, which is well below typical efficiencies for conventional compressors. It was argued that COP improvements of 5% to 18% can be reached if a well designed compressor is used. The experimental measurements did not compare very well with the simulation model (Trutassanawin, 2006), which was attributed to the lack of a correlation for accurately predicting the quality-based heat transfer coefficient in the cold-plate microchannel heat sink for the refrigerant boiling heat transfer. It was recommended that more accurate correlations to predict the refrigerant flow boiling heat transfer coefficient and better designs of miniature compressors targeted specifically for electronics cooling are needed to improve the system performance. While Bertsch et al. (2008) focus on the former recommendation, this paper discusses development and optimization of the miniature compressor.

The maximum dimensions, possible compressor shapes, and their respective physical volumes for an 80 W cooling application of a notebook computer are shown in Figure 2. These parameters are based on industry recommendations. It is believed that compressors of this size as part of the refrigeration system can fit inside the notebook computer to provide cooling for most of the contemporary processors. Performance requirements and design parameters for the miniature refrigeration cycle are listed in Table 1. Due to its high theoretical COP, medium pressure rise and volume flow rate, non-flammability, and zero ozone depletion potential, refrigerant R134a seems well suited for this application. In addition, two relatively new HFC refrigerants, namely R236fa and R245fa, that also exhibit the above characteristics, are considered in this analysis as well. Based on a thermodynamic cycle analysis using these refrigerants, the pressure rise and flow rate requirements for refrigeration cycles working with these three refrigerants are also listed in Table 1.

An electrostatically actuated diaphragm compressor offers promise for the miniature cooling system application because of its potential for high efficiency, compactness and scalability. The diaphragm compressor, schematically represented in Figure 3, consists of a flexible circular diaphragm clamped at its circumference, enclosed by two identical halves of a conformal chamber. Gas is admitted into the chamber through the suction ports at it circumference while the discharge valves control discharge flow and pressure rise. Metallic electrode layers are deposited on the diaphragm and on the chamber surfaces and dielectric layers are deposited on the top of the metallic electrodes to prevent electrical shorting when the diaphragm touches the chamber surface. The principle of operation of the diaphragm compressor is based on the progressive electrostatic zipping of the diaphragm towards the chamber when a DC potential difference is applied between them. The diaphragm compressor has been analytically modeled by the authors (Sathe et al., 2008). A model validation with the literature and with the experimental results using a custom test setup has also been presented. While the diaphragm compressor model was illustrated using a sample set of geometric design parameters, the effects of varying the chamber dimensions on the overall performance of the diaphragm compressor were not considered. For a potential application in electronics cooling, an optimized design of the diaphragm compressor that offers the best performance at the lowest compression power is required. Using the analytical model developed by Sathe et al. (2008) as the basis, an

optimization study for the diaphragm compressor is presented in this paper. Similar studies can be conducted for other types of compressors.

2. PRESSURE RISE – VOLUME FLOW RELATIONSHIP

The analytical diaphragm compressor model developed by Sathe et al. (2008) predicts the required pull-down voltage for achieving a specified pressure rise. While the dielectric properties of the dielectric layer on the chamber limits the maximum pull-down voltage for the compressor, the maximum pressure rise achieved in the chamber is limited by the geometric and elastic properties of the diaphragm. The diaphragm stress analysis in Sathe et al. (2008) indicates that this maximum chamber pressure rise allowed by the elastic deformation of the diaphragm is given as:

$$\Delta P_{\max} = f(R, w, E, \beta, \sigma) \tag{1}$$

Plastic deformation of the diaphragm beyond its elastic limit of 3% (DuPont, 2006) is irreversible, therefore undesirable. The maximum possible pressure rise in the chamber as a function of the chamber radius for different diaphragm thicknesses is plotted in Figure 4. Based on the trends, the maximum sustainable pressure increases as the chamber radius decreases and vice versa. The volume flow rate of the compressor is a function of the chamber volume and the pumping frequency as shown below:

$$\dot{V} = Vol_{chamber} \cdot Freq \cdot \eta_{Vol} \tag{2}$$

The chamber swept volume is given as:

$$Vol_{chamber} = 4 \cdot \pi \cdot R^2 \cdot Y \cdot \int_0^1 y(r) \cdot r \cdot dr \tag{3}$$

where Y is the maximum depth of the chamber given in terms of the chamber radius and the aspect ratio (AR) as:

$$Y = \frac{R}{AR} \tag{4}$$

The term $y(r)$ in Equation (3) is the non-dimensional equation representing the chamber profile. Based on Equation (3), the chamber volume varies with the square of the chamber radius. Hence, the volume flow rate increases as the chamber radius increases and vice versa. Based on Equations (1) and (2), the compressor pressure rise and volume flow rate are related to the chamber geometry as follows:

$$\Delta P \propto \frac{1}{R^2}$$
$$\dot{V} \propto R^3 \tag{5}$$

Using the design parameters described in Table 2, the relations developed in Equation (5) are graphically shown in Figure 5 where the chamber pressure rise and refrigerant volume flow rate are plotted as a function of the chamber radius. Indeed, as the chamber radius is increased, the pressure rise decreases while the volume flow rate increases. This reflects an inherent trade-off between these two parameters (Figure 6). Any design strategies focused on enhancing the pressure rise would result in a decrease in volume flow rate and vice versa. Since these two parameters are independent of each other, a design optimization that would maximize the performance of the compressor is needed, which is presented in the next section.

3. COMPRESSOR PERFORMANCE OPTIMIZATION

Based on the previous discussion, it can be argued that the optimization point for the diaphragm compressor must lie within the limits illustrated in Figure 5. The first optimization strategy involves minimizing the thermodynamic compression power for the compressor. As stated above, the most important performance parameters of the compressor, pressure rise and volume flow rate are physically independent of each other. To account for both of these parameters, the compression power has been chosen as an optimization variable. While it cannot be considered as the actual power input to the compressor, it is argued that minimizing the compression power will

make the compressor thermodynamically more efficient. Compression power for a polytropic compression process is given as (Moran and Shapiro, 2006):

$$\dot{W}_{ther} = \frac{n \cdot v_{suc} \cdot \dot{V} \cdot \bar{R} \cdot T_{suc}}{n-1} \cdot \left[1 - \left(\frac{P_{dis}}{P_{suc}} \right)^{\frac{n-1}{n}} \right] \quad (6)$$

where n = 1.178 and $\bar{R}$ = 81.49 J kg^{-1} K^{-1} for the refrigerant R134a. The compressor discharge pressure (P_{dis}) is the sum of the suction pressure and chamber pressure rise as:

$$P_{dis} = P_{suc} + \Delta P \quad (7)$$

Using the chamber pressure rise estimated in Figure 5 in Equation (6), a variation of the theoretical compression work with the chamber radius is plotted as shown in Figure 7. The compression work slightly drops as the radius of the chamber is increased. After reaching a minimum (30.1 mW), it increases rapidly with further increase in the chamber radius. This can be explained based on Equation (5). The chamber radius (R_1) corresponding to the minimum thermodynamic compression work is approximately 8.5 mm.

For an electrostatically actuated diaphragm compression, another important design parameter, in addition to the pressure rise and the volume flow rate, is the required diaphragm pull-down voltage. Higher operating voltages are undesirable because of the required increase in the dielectric layer thickness. A detailed analytical approach for calculating the pull-down voltage for the given chamber geometry and the chamber pressure rise is described by Sathe et al. (2008). Based on this analysis, the pull-down voltage for the diaphragm compressor can be expressed as:

$$D \propto \frac{Y}{R} \cdot \sqrt{\Delta P} \quad (8)$$

Using a dome-shaped chamber geometry and the diaphragm and dielectric properties listed in Table 2, the pull-down voltage is calculated as a function of the chamber radius as shown in Figure 8. The pull-down voltage initially decreases, reaches a minimum and then increases with a further increase in the chamber radius. The minimum pull-down voltage (386.5 V) occurs at a chamber radius (R_2) of 9.5 mm.

Calculation of the pull-down voltage at radius R_1 shows that the pull-down voltage is 387.7 V, which is 0.3% higher than the pull-down voltage at radius R_2. On the other hand, calculating the thermodynamic compression power at radius R_2 gives 31.8 mW, which is 5.2% higher than that at radius R_1. Hence, radius R_1 (= 8.5 mm) is selected as the optimized chamber radius at which both variables the theoretical power and the pull-down voltage are minimum. For an aspect ratio of 100, the maximum chamber depth is estimated as 85 μm (Equation (4)). The different design parameters for the compressor chamber of this geometry are shown in Table 3. Comparing the pressure rise and volume flow rate quantities required for 80 W laptop cooling application (Table 1) and the actual deliverable quantities (Table 3), it follows that the cooling requirement cannot be satisfied by using a single diaphragm compressor unit.

4. DIAPHRAGM COMPRESSOR ARRAY

To achieve the pressure rise and refrigerant volume flow rate required for the 80 W cooling application, an array of the diaphragm compressor is proposed, where multiple units of diaphragm compressor are arranged in parallel and series to achieve the desired volume flow rate and the desired pressure rise, respectively. Cabuz et al. (1999) proposed a 3-D array of dual diaphragm pumps for enhancing the pumping rate. A similar arrangement is proposed for the present analysis. The chamber dimensions, optimized in the previous section, are used for defining the external dimensions of the individual compressor unit as shown in Figure 9. The physical external volume of the compressor unit is given as:

$$Vol_{unit} = 36 \cdot R^2 \cdot Y \quad (9)$$

In a series arrangement, the discharge of one compressor unit is passed to the suction of the other compressor unit (Figure 10 (a)). Hence, the series arrangement enhances the pressure rise. A similar arrangement for increasing the

pressure rise has been proposed by Yoon (2006). Neglecting the pressure drop in the piping, for *M* compressor units in series, the net pressure rise of the arrangement is given as:

$$\Delta P_{net} = M \cdot \Delta P_{unit} \tag{10}$$

A parallel arrangement, on the other hand, involves arranging each compressor unit such that the pressure rise achieved is the same, but the volume flow rate is increased (Figure 10 (b)). The volume flow rate for an arrangement with *N* compressor units in parallel is given as:

$$\dot{V}_{net} = N \cdot \dot{V}_{unit} \tag{11}$$

It follows that for generating the necessary pressure rise and volume flow rate for the 80 W cooling capacity (Table 1), a 3-D array with *M* units in series and *N* units in parallel is required. The external physical volume of the array is given as:

$$Vol_{net} = U \cdot Vol_{unit} \tag{12}$$

where *U* is the total number of compressor units required and is a product of *M* and *N*. Using Table 1, Table 3 and Equations (9) through (12), the number of required compressor units in series (*M*), in parallel (*N*) and the external physical volume of the *M* x *N* array (Vol_{net}) are calculated and summarized in Table 4 and also shown graphically in Figure 11. For the given application, 3-D compressor arrays of 172, 104 and 126 diaphragm compressors are needed to make up the required pressure rise and volume flow rate using refrigerants R134a, R236fa and R245fa, respectively. The calculated volumes of the diaphragm compressor arrays are compared with the available volume for the compressor (Figure 2). The comparison indicates that it is theoretically possible to fit 3-D compressor arrays using any of these refrigerants within the volume constraints of 32 cm^3.

5. CONCLUSIONS

An optimization procedure for an electrostatically actuated diaphragm compressor for application in electronics cooling is studied. The diaphragm compressor simulation model developed previously has been used for this study. The maximum pressure differential achieved in the diaphragm compressor is observed to be a function of the maximum strain the diaphragm can handle before it reaches the elastic limit. A correlation between the pressure rise and the volume flow rate shows that the two are inversely proportional to each other. Hence, to achieve a trade-off, two different optimization strategies, i.e. minimizing the theoretical compression work and minimizing the required pull-down voltage for the compressor, are analyzed. Based on the optimization results, the dimensions of the diaphragm compressor are selected that are used for estimating the external volume occupied by the compressor. Three different refrigerants are used in the study and since a single unit is not capable of fulfilling the need of 80 W cooling capacity, a 3-D array of diaphragm compressors is proposed. Based on the optimized dimensions, an external volume of the compressor array is constructed and it is shown that it is possible to fit it within the specified volume constraints of 32 cm^3 using any of the three refrigerants.

While the fabrication complexities and associated cost for such a compressor array have not been considered in this analysis, it is believed that with rapid advances in the silicon micro-fabrication techniques, the diaphragm compressor holds promise. Moreover, the present analysis also serves as an analytical optimization tool that can be customized based on the type of the pumping device chosen.

ACKNOWLEDGEMENT

The authors acknowledge financial support for this work from members of the Cooling Technologies Research Center, a National Science Foundation Industry/University Cooperative Research Center at Purdue University.

NOMENCLATURE

Symbols:		Symbols:	
AR	Chamber aspect ratio	w	Diaphragm thickness (μm)
COP	Coefficient of performance	Y	Maximum chamber depth (μm)
D	Applied DC voltage (V)		
E	Elastic modulus of diaphragm (GPa)		
$Freq$	Diaphragm actuation frequency (Hz)	Greek:	
M	Number of compressors in series	β	Diaphragm Poisson's ratio
N	Number of compressors in parallel	σ	Initial stress in diaphragm (MPa)
n	Polytropic compression index	ΔP	Pressure rise in the chamber (kPa)
R	Chamber radius (mm)	η_{Vol}	Volumetric efficiency of compressor
$\overline{R}$	Specific gas constant (J kg^{-1} K^{-1})		
T	Temperature (K)		
U	Number of units in a compressor array	Subscripts:	
$\dot{V}$	Volume flow rate (ml min^{-1})	dis	Discharge
Vol	Volume (cm^3)	suc	Suction
v	Refrigerant specific volume (m^3 kg^{-1})	$ther$	Thermal
$\dot{W}_{ther}$	Theoretical compression work (mW)		

REFERENCES

Bash, C. E., 2001. Analysis of Refrigerated Loops for Electronics Cooling. Proc of IPACK'01 The Pacific Rim/ASME International Electronic Packaging Technical Conference and Exhibition, Kauai, Hawaii. 811-819.

Bertsch, S. S., Groll, E. A., Garimella, S. V., 2008. Refrigerant flow boiling heat transfer in parallel microchannels as a function of local vapor quality. Int. Journal of Heat and Mass Transfer, doi:10.1016/j.ijheatandmasstransfer.2008.01.026.

Cremaschi, L., Groll, E. A., Garimella, S. V., 2007. Performance potential and challenges of future refrigeration-based electronics cooling approaches. Proceedings of THERMES 2007. Santa Fe, New Mexico, USA.

DuPont, Inc., 2006. DuPont kapton HN polyimide film data sheet. http://www2.dupont.com/Kapton/en_US/assets/downloads/pdf/HN_datasheet.pdf.

Garimella, S. V., 2006. Advances in mesoscale thermal management technologies for microelectronics. Microelectronics Journal 37 (11), 1165-1185.

Heydari, A., 2002. Miniature Vapor Compression Refrigeration Systems for Active Cooling of High Performance Computers. The 8th Intersociety Conference on Thermal and Thermomechanical Phenomena in Electronic Systems (I-THERM). 371-378.

Krishnan, S., Garimella, S. V., Chrysler, G. M., Mahajan, R. V., 2007. Towards a thermal Moore's law. IEEE Transactions on Advanced Packaging 30 (3), 462-474.

Mongia, R., Masahiro, K., DiStefano, E., Barry, J., Chen, W., Izenson, M., Possamai, F., and Zimmermann, A., 2006. Small scale refrigeration system for electronic cooling within a notebook computer. ITHERM 2006, 0-7803-9524, 751-758.

Moran, M. J., Shapiro, H. N., 2004. Fundamentals of engineering thermodynamics. John Wiley and Sons, Inc. Hoboken, New Jersey, USA.

Phelan, P. E., 2001. Current and future miniature refrigeration cooling technologies for high power microelectronics. Semiconductor Thermal Measurement and Management Symp.: 17th Annual IEEE, San Jose, CA. 158-167.

Sathe, A. A., Groll, E. A., Garimella, S. V., 2008. Analytical Model for an Electrostatically Actuated Miniature Diaphragm Compressor. Journal of Micromechanics and Microengineering, 18 (3), # 035010.

Trutassanawin, S., 2006. A miniature-scale refrigeration system for electronics cooling. Ph.D. Thesis. School of Mechanical Engineering, Purdue University, West Lafayette, USA.

Trutassanawin, S., Groll, E. A., Garimella, S. V. and Cremaschi, L., 2006. Experimental investigation of a miniature-scale refrigeration system for electronics cooling. IEEE Transactions on Components and Packaging Technologies, 29 (3), 678-687.

Yoon, J. S., 2006. Studies on the micro vapor compressor for the application to a miniature refrigeration system. PhD thesis, School of Mechanical and Aerospace Engineering, Seoul National University, South Korea.

Table 1. Design parameters for the miniature refrigeration system using three refrigerants.

Requirements:			
• System cooling capacity	80 W		
• Evaporator temperature	20 °C		
• Suction superheat	5 K		
• Condenser temperature	35 °C		
• Condenser subcooling	5 K		
• Compressor overall isentropic efficiency†	65%		
• Compressor volumetric efficiency†	90%		
Calculations:	R134a	R236fa	R245fa
• Suction pressure [kPa]	572	230	124
• Discharge pressure [kPa]	888	376	213
• Pressure rise (ΔP_{net}) [kPa]	316	146	89
• Volume flow rate ($\dot{V}_{net}$) [ml min^{-1}]	1141	2496	4119

† - Assumed for this analysis

Table 2. Design parameters for the diaphragm compressor.

Chamber profile	Dome-shaped (Sathe et al., 2008)
Chamber aspect ratio (*AR*)	100
Dielectric thickness on chamber surface	1 μm
Dielectric constant	3.5
Diaphragm material	Kapton (DuPont, 2006)
Diaphragm thickness (w)	25 μm
Diaphragm elastic modulus (*E*)	3 GPa
Diaphragm Poisson's ratio (ν)	0.3
Diaphragm initial stress (σ)	15 MPa
Pumping frequency (*Freq*)	90 Hz

Table 3. Design parameters for the optimized diaphragm compressor.

Chamber radius	8.5 mm
Maximum chamber depth	85 μm
Maximum pressure rise	35.6 kPa
Volume flow rate	97 ml min^{-1}
Pull-down voltage	387 V

Table 4. Details of the proposed diaphragm compressor array using three refrigerants.

Refrigerant	R134a	R236fa	R245fa
Number of units in series*	16	4	3
Number of units in parallel*	12	26	42
Total number of units	172	104	126
External volume of single unit [cm^3]	0.221	0.221	0.221
External volume of the array [cm^3]	31.84	22.98	27.85
Available external volume [cm^3]	32	32	32

* – Numbers rounded to the closest decimal

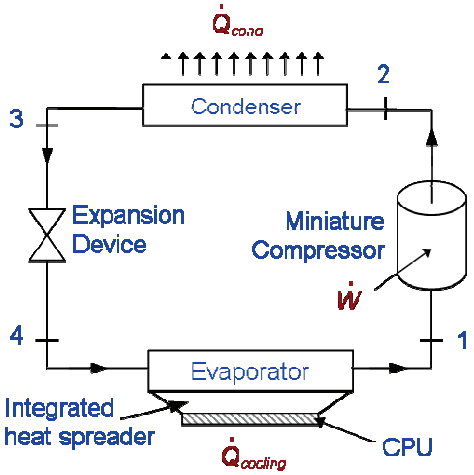

Figure 1. Schematic of a miniature refrigeration system for electronics cooling.

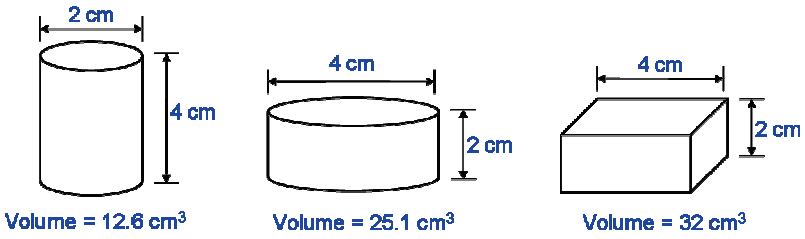

Figure 2. Possible compressor shapes and dimensions for 80 W notebook computer cooling application.

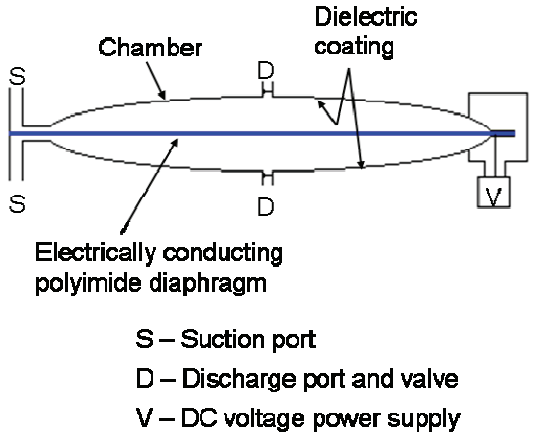

Figure 3. Schematic of an electrostatically actuated diaphragm compressor.

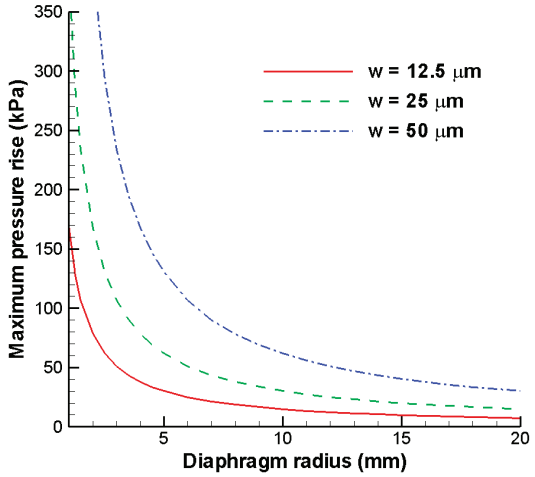

Figure 4. Maximum sustainable pressure rise for different radii (R) and thicknesses (w) of the diaphragm.

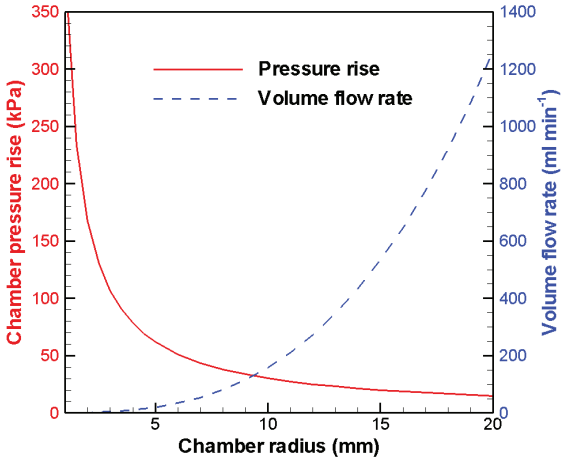

Figure 5. Chamber pressure rise and refrigerant volume flow rate versus chamber radius.

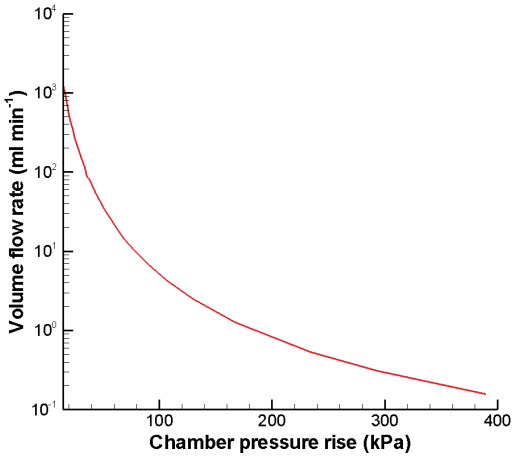

Figure 6. Refrigerant volume flow rate versus chamber pressure rise.

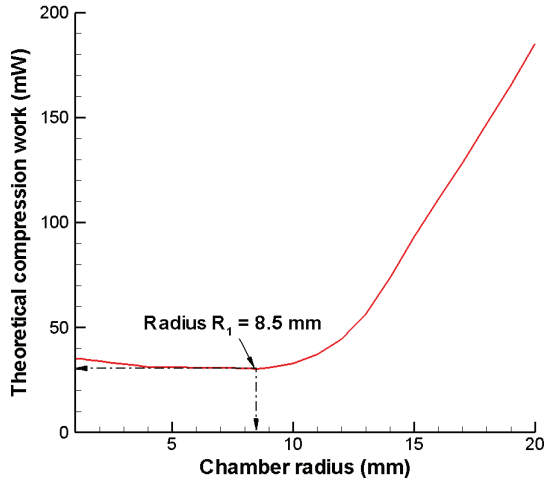

Figure 7. Theoretical compression work for R134a versus chamber radius (Optimum chamber radius R_1 = 8.5 mm).

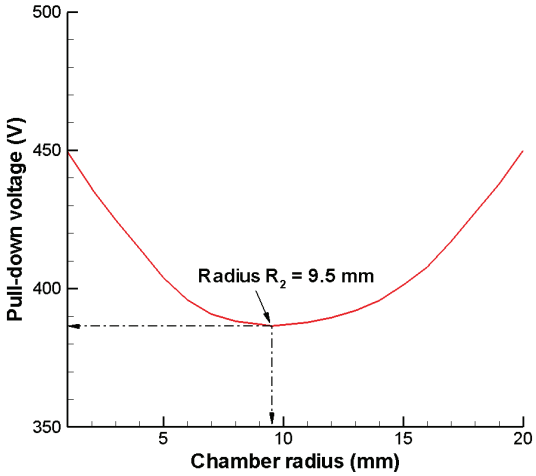

Figure 8. Pull-down voltage for R134a versus chamber radius (Optimum chamber radius R_2 = 9.5 mm).

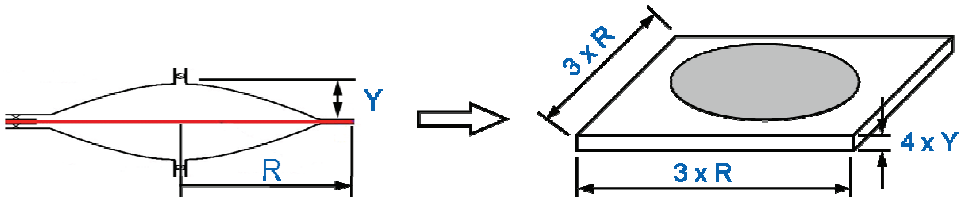

Figure 9. Defining external dimensions of the diaphragm compressor unit as a function of the chamber dimensions (Not to scale).

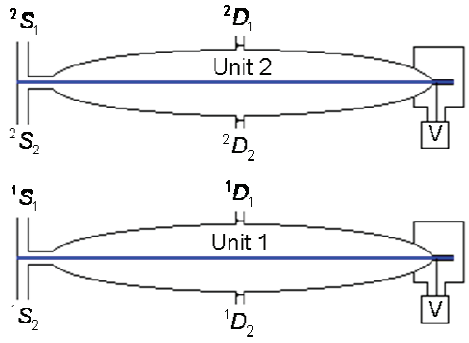

From	To
Suction manifold	$^1S_1$ and $^1S_2$
$^1D_1$	$^2S_1$
$^1D_2$	$^2S_2$
$^2D_1$ and $^2D_2$	Discharge manifold

(a)

From	To
Suction manifold 1	$^1S_1$ and $^1S_2$
Suction manifold 2	$^2S_1$ and $^2S_2$
$^1D_1$ and $^1D_2$	Discharge manifold 1
$^2D_1$ and $^2D_2$	Discharge manifold 2

(b)

Figure 10. Schematic of two diaphragm compressor units (a) in series for enhancing the pressure rise, and (b) in parallel for enhancing the volume flow rate.

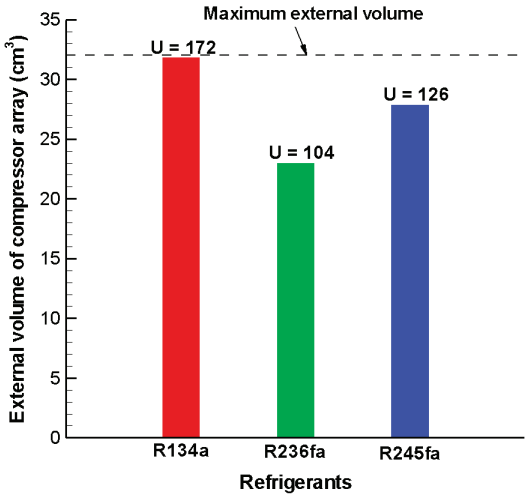

Figure 11. Comparison of external volumes of the compressor arrays using different refrigerants with total number of units required given as *U*.